

# An activating mutation in the *CSF3R* gene induces a hereditary chronic neutrophilia

Isabelle Plo,<sup>1,2,3</sup> Yanyan Zhang,<sup>1,2,3</sup> Jean-Pierre Le Couédic,<sup>1,2,3</sup>  
 Mayuka Nakatake,<sup>1,2,3</sup> Jean-Michel Boulet,<sup>4</sup> Miki Itaya,<sup>5</sup> Steven O. Smith,<sup>5</sup>  
 Najet Debili,<sup>1,2,3</sup> Stefan N. Constantinescu,<sup>6,7</sup> William Vainchenker,<sup>1,2,3</sup>  
 Fawzia Louache,<sup>1,2,3</sup> and Stéphane de Botton<sup>1,2,3,8</sup>

<sup>1</sup>Research Laboratory on Hematopoiesis and Normal and Leukemic Stem Cells, U790, Institut National de la Santé et de la Recherche Médicale, 94805 Villejuif, France

<sup>2</sup>Université Paris-Sud 11, 94805 Villejuif, France

<sup>3</sup>Institut Gustave Roussy, Institut Fédératif de Recherche 34, 94805 Villejuif, France

<sup>4</sup>Centre Hospitalier Régional Orléans, Hôpital de la Source, 45000 Orléans, France

<sup>5</sup>Department of Biochemistry and Cell Biology, Center for Structural Biology, Stony Brook University, Stony Brook, NY 11794

<sup>6</sup>Ludwig Institute for Cancer Research, 1200 Brussels, Belgium

<sup>7</sup>de Duve Institute, Université Catholique de Louvain, 1200 Brussels, Belgium

<sup>8</sup>Department of Hematology, Institut Gustave Roussy, 94805 Villejuif, France

**We identify an autosomal mutation in the *CSF3R* gene in a family with a chronic neutrophilia. This T617N mutation energetically favors dimerization of the granulocyte colony-stimulating factor (G-CSF) receptor transmembrane domain, and thus, strongly promotes constitutive activation of the receptor and hypersensitivity to G-CSF for proliferation and differentiation, which ultimately leads to chronic neutrophilia. Mutant hematopoietic stem cells yield a myeloproliferative-like disorder in xenotransplantation and syngenic mouse bone marrow engraftment assays. The survey of 12 affected individuals during three generations indicates that only one patient had a myelodysplastic syndrome. Our data thus indicate that mutations in the *CSF3R* gene can be responsible for hereditary neutrophilia mimicking a myeloproliferative disorder.**

## CORRESPONDENCE

William Vainchenker:  
 verpre@igr.fr

Abbreviations used: G-CSF-R, G-CSF receptor; HSC, hematopoietic stem cell; MPD, myeloproliferative disorder; qRT-PCR, quantitative real-time PCR; SCF, stem cell factor; TM, transmembrane; TPO, thrombopoietin.

Hereditary erythrocytosis and thrombocytosis with an autosomal-dominant pattern are linked to mutations in the erythropoietin or thrombopoietin (TPO; MPL) receptors (de la Chapelle et al., 1993; Kralovics et al., 1997; Ding et al., 2004), respectively, or to a dysregulation of the synthesis of these two cytokines (Wiestner et al., 1998). These syndromes differ from classical myeloproliferative disorders (MPDs) by the low incidence of early and late complications. They recapitulate the chronic administration of recombinant growth factors (i.e., TPO and erythropoietin). The G-CSF receptor (G-CSF-R) is also a type I cytokine receptor that binds G-CSF, the main cytokine that regulates granulopoiesis. G-CSF-R activation by G-CSF not only induces proliferation and differentiation of neutrophils but also mobilizes BM hematopoietic progenitors cells to blood (Panopoulos and Watowich, 2008). In this report, we identified a familial chronic neutrophilia caused by an

autosomal-dominant *CSF3R* gene mutation that constitutively activates G-CSF-R.

## RESULTS AND DISCUSSION

We studied a three-generation Caucasian pedigree (aged 8–80 yr; Fig. 1 A) in which 12 out of 16 individuals (6 males and 6 females) presented with a chronic neutrophilia associated with splenomegaly. The disorder was discovered in patient 15 during a unique episode of systemic inflammatory response syndrome that combined fever, tachycardia, dyspnea, pleural and pericardial effusion, hepatosplenomegaly, and weight loss. Biological features associated increased WBC counts by 102,000 cells/mm<sup>3</sup>, with 75% segmented neutrophils and 20% immature granulocytes, the hemoglobin level by 10 g/dl, and the platelet count by 101,000

I. Plo and Y. Zhang contributed equally to this paper.

© 2009 Plo et al. This article is distributed under the terms of an Attribution-Noncommercial-Share Alike-No Mirror Sites license for the first six months after the publication date (see <http://www.jem.org/misc/terms.shtml>). After six months it is available under a Creative Commons License (Attribution-Noncommercial-Share Alike 3.0 Unported license, as described at <http://creativecommons.org/licenses/by-nc-sa/3.0/>).

cells/mm<sup>3</sup>. BM analysis revealed an increase in granulocyte precursors without an excess of blasts. Karyotype was normal. *Bcr-Abl* transcripts and *JAK2V617F* were not detected. After this episode, patient 15 returned to chronic neutrophilia, but 18 mo later, he developed a myelodysplastic syndrome (refractory anemia with an excess of blasts type I) associating pancytopenia (hemoglobin, 8.1 g/dl; platelets, 41,000 cells/mm<sup>3</sup>; 800 polymorphs per mm<sup>3</sup> along with 12% of circulating immature granulocytes), skin infiltration by mature granulocytes, and 9% BM blasts. BM aspirate examination also showed a marked dysgranulopoiesis but no dyserythropoiesis or dysmegakaryopoiesis. A clonal abnormality (del 3q26) was detected by a conventional cytogenetic in 70% of the metaphases

(14 out of 20). A fluorescent in situ hybridization analysis did not show evidence of *EVI1* rearrangement (De Melo et al., 2008). To eliminate a transcriptional activation of *EVI1*, we performed quantitative real-time PCR (qRT-PCR). A 30% decrease in *EVI1* mRNA was detected (Fig. S1), suggesting that the deletion includes this gene.

Familial history showed that 12 out of 16 members had a chronic neutrophilia. There was no evidence of consanguinity in this pedigree. In the 12 patients, median WBC counts were 21,350 cells/mm<sup>3</sup> (range: 14,900–32,800 cells/mm<sup>3</sup>) in peripheral blood, with >70% segmented neutrophils or band cells and <10% immature granulocytes. Median neutrophil counts were 16,900 cells/mm<sup>3</sup> (range: 11,000–23,700

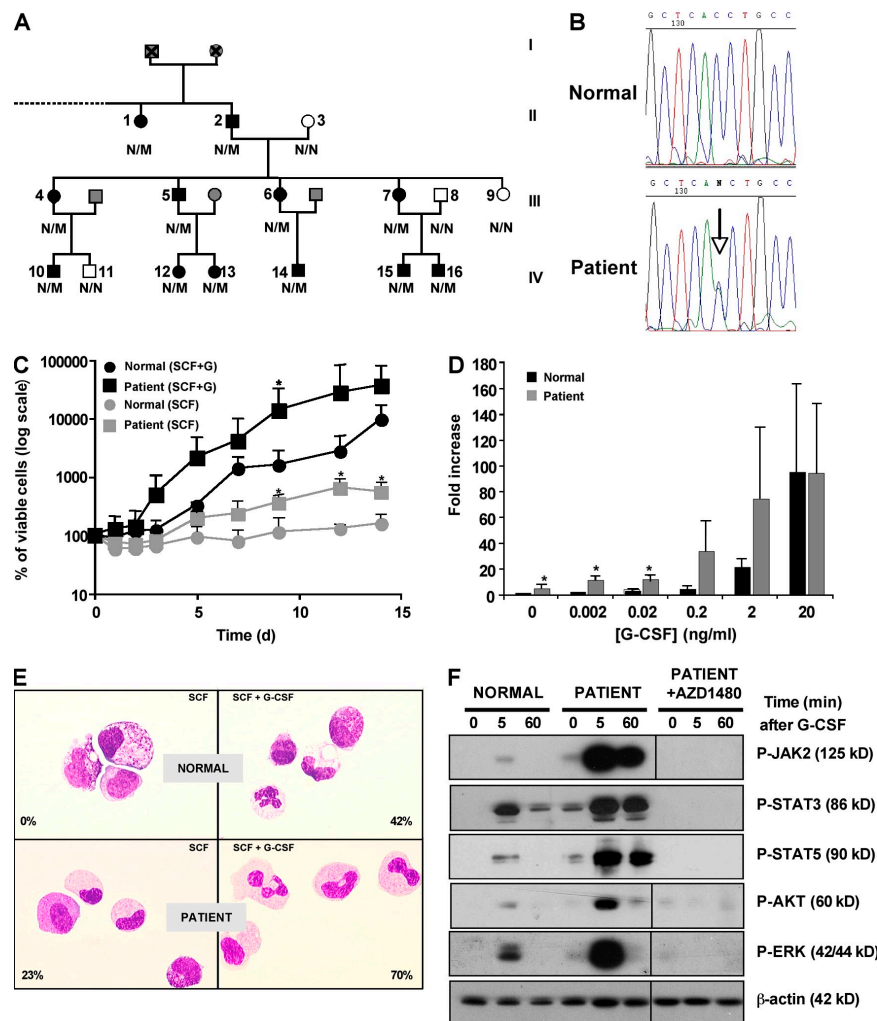


**Figure 1. An inherited mutation in the *CSF3R* gene in a familial neutrophilia.** (A) Pedigree of the family. The black symbols represent affected individuals with neutrophilia and T617N amino acid substitution. The gray symbols represent individuals for whom clinical information was not available. The white symbols represent nonaffected individuals. The genotype is also indicated (N/N, normal subjects; N/M, heterozygous patients). (B) Examples of electrophoreograms from normal subjects or patient 15 DNA (T617N). (C–E) Liquid culture of CD34<sup>+</sup> cells in the presence of SCF plus G-CSF (C and D) from controls ( $n = 5$ ) or patients ( $n = 2$ , patients 7 and 15) in which three independent experiments were performed for each patient. Error bars represent means  $\pm$  SD. \* $P < 0.05$ . (E) Cytological examination at day 21 of culture. Numbers indicate the percentages of mature granulocytic cells. Results are representative of controls ( $n = 3$ ) or patients ( $n = 2$ , patients 7 and 15) in which two independent experiments were performed for each patient. (F) Western blot analysis of P-JAK2, P-STAT3, P-STAT5, P-ERK p42-p44, and P-AKT antibodies in normal or patient CD34<sup>+</sup> cells stimulated by G-CSF in the presence or not of AZ1480. Results are representative of three independent experiments either with control or patient 15. Black lines indicate that intervening lanes have been spliced out.

cells/mm<sup>3</sup>). In the peripheral blood, a 3- to 20-fold increase in the percentage of circulating CD34<sup>+</sup> cells was observed (Table I). The BM of two analyzed affected individuals contained an increase in granulocyte precursors without an excess of blasts. The karyotype was normal; *Bcr-Abl* transcripts and *JAK2*<sup>V617F</sup> were not detected. All affected patients except patient 15 had no clinical symptoms.

Based on the autosomal-dominant pattern of inheritance of the disorder and the high level of blood CD34<sup>+</sup> cells, we tested the hypothesis that neutrophilia in this family resulted from activation of the G-CSF-R signaling. Because G-CSF concentration in the serum (two patients studied) was below the detection limit (<39 pmol/ml), we sequenced the *CSF3R* gene. We found a heterozygous C-to-A substitution at nucleotide 2,088 that leads to a threonine-to-asparagine substitution (T617N; Fig. 1 B). This heterozygous point mutation was observed in the 12 affected individuals but not in the 4 healthy family members, and was segregated with the neutrophilia (Fig. 1 A). Moreover, the mutation was found in all generations and in as many affected men as women. Finally, the mutation was transmitted with an autosomal-dominant pattern of inheritance with complete penetrance. The *CSF3R*<sup>T617N</sup> mutation has already been described as an activating mutation found in 2 out of 555 patients with acute myeloid leukemia (Forbes et al., 2002). In these two cases, the mutation was acquired because it disappeared after complete remission achievement and was not detected at relapse (Forbes et al., 2002). This last result demonstrates that the *CSF3R*<sup>T617N</sup> mutation was a secondary event in the leukemic process. We studied whether this mutation could be found in sporadic cases of unexplained neutrophilia and investigated 40 cases by allele-specific PCR, but we did not find any other positive case suggesting that this activating mutation is rare.

The *G-CSF-R*<sup>T617N</sup> mutation is located in the transmembrane (TM) domain of the receptor, analogously to the *MPL*<sup>S505N</sup>

mutation associated with hereditary or acquired thrombocytopenia (Ding et al., 2004; Chaligne et al., 2008). To evaluate the influence of the T617N mutation on TM helix interactions in the G-CSF-R, conformational searches were performed to identify low energy dimer conformations (Adams et al., 1996). For the wild-type G-CSF-R sequence, the lowest energy dimer structure that emerged from the searches had a symmetric orientation of the TM helices with Thr617 in the interface. The lowest energy structures of T617N G-CSF-R dimers had the same helix orientation, but with substantially lower interaction energies (wild-type, approximately −69 kcal/mol; T617N mutant, approximately −81 kcal/mol; Fig. 2). These computational data strongly support the notion that Asn617 stabilizes an active dimeric orientation for G-CSF-R by forming interhelical hydrogen bonds.

To determine the impact of the mutant G-CSF-R<sup>T617N</sup> on G-CSF sensitivity, we measured granulocytic proliferation and differentiation from CD34<sup>+</sup> cells in in vitro experiments. In the presence of stem cell factor (SCF) and G-CSF, proliferation was not significantly different between normal subjects and affected patients (patients 7 and 15). In contrast, SCF alone induced survival of control CD34<sup>+</sup> cells, whereas it elicited proliferation (4.3-fold) on patient cells (Fig. 1 C). We also observed a hypersensitivity to G-CSF of patient CD34<sup>+</sup> cells (Fig. 1 D) that was confirmed by clonogenic assays in methylcellulose (Fig. S2). Moreover, when CD34<sup>+</sup> cells from normal subjects and affected individuals were grown in the presence of G-CSF, cells differentiated into mature granulocytes, as indicated by cytological examination (Fig. 1 E). In contrast, in the presence of SCF alone, only cells from patients acquired the terminal granulocytic CD11b antigen (Fig. S3) and matured into neutrophilic polymorphs (Fig. 1 E). Collectively, these results show that mutant G-CSF-R<sup>T617N</sup> induces a G-CSF-independent granulocytic proliferation and differentiation.

**Table I.** Laboratory hematological values from the family members

Numbers	Age	WBCs (per mm <sup>3</sup> )	Neutrophils (per mm <sup>3</sup> )	Hemoglobin	Platelets (per mm <sup>3</sup> )	Circulating CD34 <sup>+</sup> (per ml)	Circulating CD34 <sup>+</sup>	Splenomegaly
	yr			g/dl			%	
1	70	14,700	11,000	13.7	157,000	NS	NS	NS
2	80	15,900	13,900	14.2	268,000	NS	NS	Yes
4	46	27,100	21,510	13.8	278,000	NS	NS	Yes
5	40	29,100	20,370	14.2	290,000	NS	NS	NS
6	35	20,400	15,700	12	267,000	NS	NS	NS
7	45	27,600	22,900	13.5	238,000	3,700	0.02	Yes
9	46	7,800	3,510	14.4	339,000	NS	NS	NS
10	19	14,900	9,700	14.7	208,000	NS	NS	NS
12	13	20,600	15,500	13.3	347,000	NS	NS	NS
13	11	21,100	14,300	13.1	474,000	NS	NS	NS
14	8	21,600	18,100	12.4	278,000	NS	NS	NS
15	20	32,800	22,300	12.8	103,000	292,000	1.29	Yes
16	11	30,400	23,700	12.9	263,000	2,800	0.01	Yes

NS, not studied.

To investigate the effects of the T617N mutation on G-CSF-R signaling, CD34<sup>+</sup> cells isolated from normal donors or patients were first deprived of cytokines, and then stimulated with G-CSF for various periods of time and subjected to Western blot analysis using specific antibodies. Interestingly, patient cells exhibited constitutive phosphorylation of JAK2, STAT3, AKT, and ERK. After G-CSF stimulation, JAK2, STAT3, STAT5, ERK, and AKT were rapidly and transiently activated in cells from normal donors, whereas phosphorylation was much more potent and sustained in cells from patients (Fig. 1 F). In addition, a specific JAK2 inhibitor abrogated constitutive and G-CSF-induced activation, suggesting that the mechanism of neutrophilia was JAK2 dependent, reminiscent of JAK2<sup>V617F</sup> MPD.

We next infected mouse lineage (Lin<sup>-</sup>) BM cells with a retrovirus containing *CSF3R*<sup>wt</sup> or *CSF3R*<sup>T617N</sup> mutation or

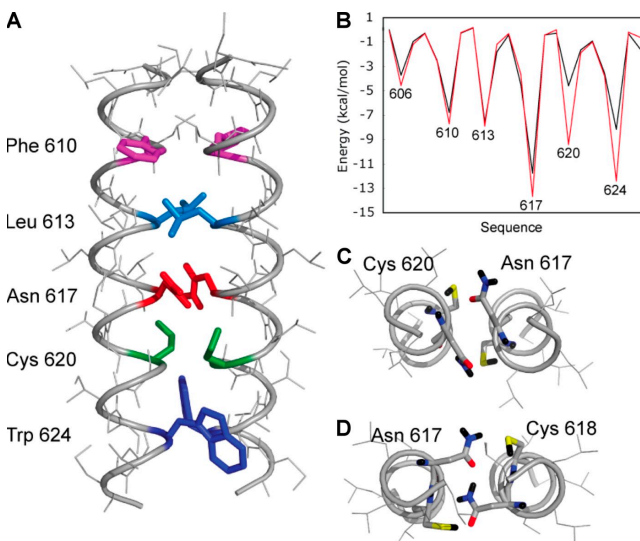


**Figure 2. Computational searches of wild-type and T617N G-CSF-R dimers.** (A) Molecular structure of the helix dimer of the T617N mutant having the overall lowest energy in the computational searches. The helices have a left-handed crossing angle and an axial separation of 10.5 Å. The interfacial amino acids are highlighted. (B) Plot of the helix interaction energies in the wild-type (black) and T617N (red) TM helix dimers with axial separations of 10.5 Å. In the wild-type G-CSF-R, the dominant interaction is a direct Thr617-Thr617 hydrogen bond between side chain hydroxyl groups. In contrast, there are several strong stabilizing interactions in the mutant. The Asn amide side chain forms hydrogen bonds to the thiol side chain of Cys620. Trp624 forms stabilizing van der Waals contacts with the opposing helix; the indole NH is also able to form an interhelical H bond with Cys620. The total interaction energies were very similar for the lowest energy T617N dimers in computational searches at 10 Å (−80.6 kcal/mol) and 10.5 Å (−81.0 kcal/mol). (C) Cross section of the T617N helix dimer showing hydrogen-bonding interactions involving Thr617 and Cys620. The axial separation is 10.5 Å. (D) Cross section of the T617N helix dimer with an axial separation of 11 Å stabilized by interhelical interactions between Asn617 side chains and between Asn617 and Cys618. The overall interaction energies were generally higher at longer interhelical separations for both the wild-type and mutant dimers, although the T617N dimers were consistently lower in energy than those of the wild-type dimers because of the ability of Asn617 to form interhelical hydrogen bonds.

the empty vector (Migr), and engrafted the infected cells into irradiated hosts. Mice transplanted with cells expressing the mutant G-CSF-R<sup>T617N</sup> developed neutrophilia and displayed a high percentage of Gr-1<sup>+</sup> granulocytes both in blood (33% in T617N vs. 15% in WT) and spleen (31% in T617N vs. 6% in WT; Fig. 3, A, B, E, and F), whereas the percentage of granulocytes in BM was only slightly affected (Fig. 3, C and D). An increase in B220<sup>+</sup> B cells was also observed in the spleen, which may be caused by an increase in lymphopoiesis mediated by the ectopic expression of the G-CSF-R<sup>T617N</sup> after retroviral transduction in hematopoietic stem cells (HSCs). Alternatively, this might be related to cytokine release in the spleen by the granulocytic precursors. All *CSF3R*<sup>T617N</sup> mice developed splenomegaly (Fig. 3 G). These data demonstrate that the T617N mutation in the G-CSF-R is at the origin of the neutrophilia observed in patients. To directly assess the consequences of this mutation on human HSCs, we performed xenotransplantation in irradiated NOG mice of CD34<sup>+</sup>

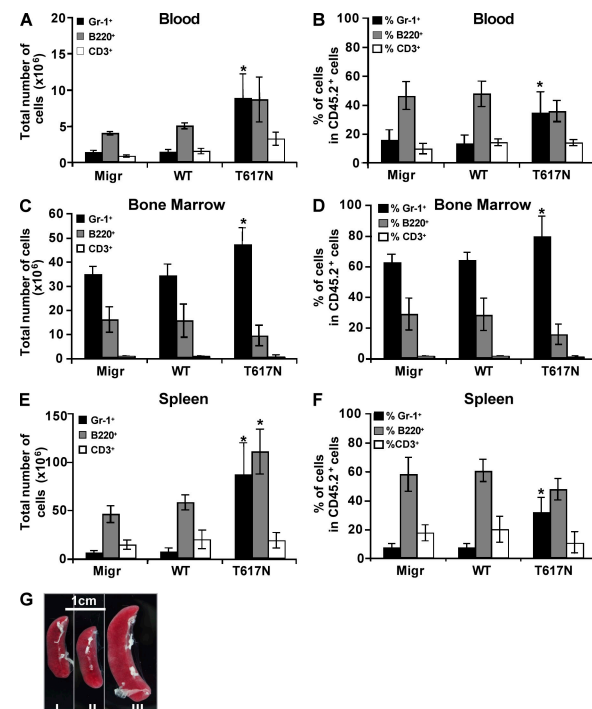


**Figure 3. *CSF3R*<sup>T617N</sup> mutation yields to MPD in the mouse BM transplant model.** BM cells were collected from C57/B6 SJL (CD45.2) mice 2 d after 5-fluorouracil treatment. Lin<sup>-</sup> cells were purified; cultured for 2 d with IL-3, SCF, IL-6, and TPO; infected twice with the viral particles containing empty vector (Migr), *CSF3R*<sup>wt</sup>, or *CSF3R*<sup>T617N</sup>; and finally injected intravenously into lethally irradiated (825 rad) C57BL6 (CD45.1) mice. After 5 wk, mice were sacrificed and the total number of cells (A, C, and E) or the percentage of cells (B, D, and F) including granulocytes (Gr-1<sup>+</sup>), B lymphocytes (B220<sup>+</sup>), or T lymphocytes (CD3<sup>+</sup>) was measured in CD45.2+ donor mouse cells in the blood (A and B), BM (C and D), and spleen (E and F). (G) Spleen from Migr-engrafted (I), *CSF3R*<sup>wt</sup>-engrafted (II), and *CSF3R*<sup>T617N</sup>-engrafted (III) mice. The results are the means ± SD of four mice of each group from two independent experiments. \*, P < 0.05 compared with Migr-engrafted mice.

cells isolated either from the blood of patient 15 or from a G-CSF–mobilized normal donor. At week 15 after transplant, the level of engraftment was measured by the percentage of human CD45<sup>+</sup> cells in mouse blood, BM, spleen, and thymus. Levels of chimerism were lower in the four organs studied when patient CD34<sup>+</sup> cells were injected compared with control cells (Fig. 4 A). Conversely, myeloid cells represented the predominant population in the blood, BM, and spleen of mice transplanted with patient CD34<sup>+</sup> cells (Fig. 4 B), whereas B cells were prevalent with control cells (Fig. 4 C), as previously described (Bhatia et al., 1997; Ito et al., 2002; Matsumura et al., 2003). This skewed differentiation of HSCs to myeloid differentiation in immunodeficient mice has previously been described in MPDs (James et al., 2008). The frequency of human myeloid progenitors found among the CD45<sup>+</sup> in the BM of mice engrafted with patient cells was increased in comparison to control cells. Moreover, a marked increase in the content of hematopoietic progenitors was observed in the blood of patient cell–engrafted mice (Fig. 4 D). Collectively, these results show that G-CSF-R<sup>T617N</sup> mutant not only skews cells to myeloid differentiation in NOG mice

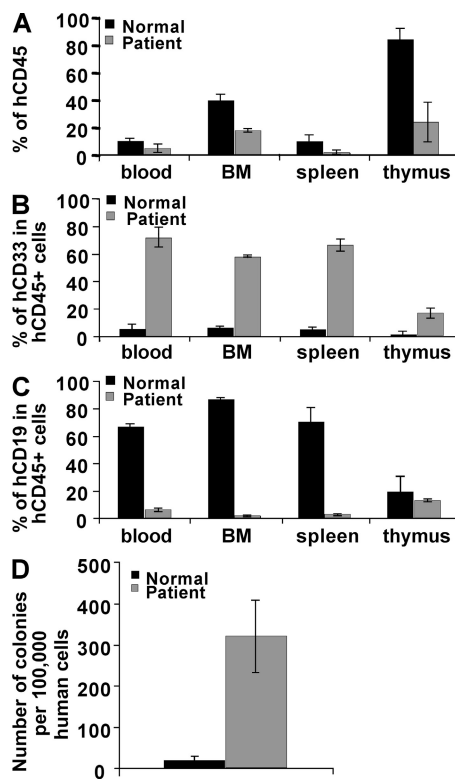


**Figure 4. *CSF3R*<sup>T617N</sup> mutation yields to MPD in the xenotransplantation model.** CD34<sup>+</sup> cells from normal subjects or from patients were intravenously injected into NOG mice and sacrificed at 15 wk. Flow cytometry analysis of human cell engraftment shows the percentage of human CD45<sup>+</sup> cells (A) and percentage of B (CD19<sup>+</sup>) and myeloid (CD33<sup>+</sup>) cells (B and C) among CD45<sup>+</sup> cells in the peripheral blood, BM, spleen, and thymus. The results are the means  $\pm$  SD of four mice for donors and patient from two independent experiments. (D) Peripheral blood progenitors among CD45<sup>+</sup> cells from donor- or patient-engrafted mice.

but also induces a mobilization of hematopoietic progenitors. Thus, in contrast to the truncating mutations found in severe congenital neutropenia, the *CSF3R*<sup>T617N</sup> mutation does not confer a major HSC-proliferative advantage but rather increases myeloid differentiation (McLemore et al., 1998; Liu et al., 2008).

In conclusion, the family described in this report is the first case of germline *CSF3R* mutation leading to a chronic neutrophilia and mobilization of hematopoietic progenitors, a phenotype similar to that induced by administration of rhG-CSF. The T617N TM mutation induces both proliferation and granulocytic differentiation. Progression to a myelodysplastic syndrome (RAEB I) malignant hemopathy was observed on 1 out of 12 affected patients. The precise role of the acquired *CSF3R* mutations found in severe congenital neutropenia is not completely resolved. Nevertheless, their association with leukemic progression is increasingly strong (Germeshausen et al., 2007; Liu et al., 2008). Therefore, more investigations are necessary to know if *CSF3R*<sup>T617N</sup> mutation predisposes to malignant myeloid hemopathies.

## MATERIALS AND METHODS

**Patient cells.** Blood samples from patients, normal subjects, and G-CSF–mobilized patients were collected after informed consent was obtained. The study was approved by the Local Research Ethics Committee from the Hôtel-Dieu and the Henri Mondor hospitals, and informed consent was obtained from each patient in accordance with the Declaration of Helsinki.

**Purification and in vitro differentiation of CD34<sup>+</sup> cells.** Mononuclear cells were separated over a Ficoll density gradient, and CD34<sup>+</sup> cells were purified by a double-positive magnetic cell sorting system (AutoMACS; Miltenyi Biotec) according to manufacturer's recommendations. CD34<sup>+</sup> cells were either plated for 15 d in methylcellulose (StemCell Technologies Inc.) in the presence of 25 ng/ml SCF and G-CSF, or amplified for 21 d in granulocytic conditions in serum-free liquid medium containing IMDM with penicillin/streptomycin/glutamine,  $\alpha$ -thioglycerol, BSA, a mixture of sonicated lipids, and insulin-transferrin in the presence of recombinant human cytokines (25 ng/ml SCF and 20 ng/ml G-CSF).

**Western blot analysis.** After purification, CD34<sup>+</sup> cells were deprived in IMDM alone for 4 h in the presence or not of JAK2 inhibitor (AZD1480) at 1  $\mu$ M. AZD1480 was a gift from AstraZeneca (Waltham, MA). Cells were stimulated by 20 ng/ml G-CSF for different intervals, washed in PBS, and lysed in denaturing loading dye buffer. Western blot analysis was performed using conventional techniques using anti-Jak2 (pY1007/1008), anti-STAT3 (pY705), anti-STAT5 (pY705), anti-ERK p42-p44 (T202/Y204), and anti-AKT (S473) antibodies (Cell Signaling Technology), and anti- $\beta$ -actin antibodies. Antibodies were visualized using the enhanced chemiluminescence detection kit (GE Healthcare).

**DNA sequencing.** Genomic DNAs were isolated from mononuclear cells or granulocytes according to standard procedures. Each of the 17 exons of the *CSF3R* gene (available from GenBank/EMBL/DDBJ under accession no. M59820) was amplified using standard PCR conditions from 300 ng of genomic DNA and primer sequences derived from flanking intronic sequences. PCR products were filtration purified (MultiScreen PCR; Millipore), sequenced using the BigDye Terminator cycle sequencing ready reaction kit (Applied Biosystems) according to the manufacturer's protocol, and analyzed on an ABI PRISM 3100 Genetic Analyzer (Applied Biosystems).

**Generation of CSF3R mutant retroviruses and in vivo reconstitution of mouse hematopoietic system.** A human hemagglutinin-tagged

full-length CSF3R open reading frame was cloned into the pMIGR-IRES-GFP retroviral vector. Mutagenesis reactions for human CSF3R were performed using the QuickChange site-directed mutagenesis kit (Agilent Technologies). All constructs were verified by sequencing.

Vesicular stomatitis virus glycoprotein-pseudotyped viral particles of pMIGR-IRES-GFP (empty vector), pMIGR-CSF3R-IRES-GFP, and pMIGR-T617N-CSF3R-IRES-GFP were produced into the 293 EBNA cells. Ecotropic virus-producing cell lines were generated from infection of the GP+E-86 packaging cell line (supplied by A. Bank, Columbia University, New York, NY) with concentrated virus supernatants.

BM ( $\text{Lin}^-$ ) cells were collected from C57BL/6 SJL (CD45.2) mice (Charles River Laboratories) 2 d after 5-fluorouracil treatment.  $\text{Lin}^-$  cells were purified; cultured for 2 d with IL-3, SCF, IL-6, and TPO; and infected twice with the viral particles and finally injected intravenously into lethally irradiated (8.25 Gy) C57BL/6 (CD45.1) mice.

Hemoglobin, mean corpuscular volume, hematocrit, RBC, platelet, and WBC counts, and the lymphocyte/granulocyte ratio were determined using an automated counter (MS9; Schloessing Melet) on blood collected from the retro-orbital plexus in citrated tubes. BM cells were removed by flushing two femurs and two tibias. Spleens were weighed and single-cell suspensions were prepared. Differential cell counts were performed after May-Grünwald-Giemsa staining of blood smears or spleen and BM cell cytopsins.

**NOG mice repopulation assays.** 24 h before transplantation, 6–8-wk-old NOD/SCID/ $\gamma\text{c}^{-/-}$  (NOG) mice, provided by M. Ito (Central Institute for Experimental Animals, Kawasaki, Japan), were sublethally irradiated (3 Gy) as previously described (Ito et al., 2002). CD34 $^+$  cells from G-CSF-mobilized donors or from patients were intravenously injected into NOG mice without any administration of cytokines. Human cell engraftment was assessed by flow cytometry by measuring human leukocytes (CD45 $^+$ ). Blood was lysed. BM cells were removed by flushing both femurs. Spleens were weighed and single-cell suspensions were prepared. NOG mice were bred in our pathogen-free breeding facility (Service Centrale d'Expérimentation Animale).

For progenitor assay, 50  $\mu\text{l}$  of peripheral blood and BM from mice engrafted with donors or patient cells were seeded in methylcellulose, and progenitors were counted after 14 d in the presence of a cocktail of cytokines (100 IU/ml IL-3, 25 ng/ml SCF, 3 IU/ml erythropoietin, and 5 ng/ml GM-CSF). The number of human colonies was normalized to 100,000 human cells.

**FACS analysis.** Flow cytometry was used to determine GFP expression and cell content of blood, BM, and spleen cells with appropriate PE- or allophycocyanin-conjugated antibodies (anti-human CD45, anti-CD45.1, anti-CD45.2, anti-CD19, anti-CD3, anti-CD33, anti-CD11b, anti-CD15, anti-CD14, anti-CD34, anti-CDB220, and anti-Gr-1 antibodies; BD) using a cytometer (FACSSort) with the Cell Quest software package (BD).

**Modeling the effect of the T617N mutation on G-CSFR structure and dimerization.** Computational searches for low energy dimer conformations were performed using the program CHI (Adams et al., 1996). Canonical helices were constructed from the TM sequence of the G-CSF-R (IILGLFGLLLTCLCGTAWLCC). Low energy conformations of helix dimers were searched by rotating each helix through rotation angles  $\varphi_1$  and  $\varphi_2$  from 0–360°, with a sampling size of 45° for axial separations between TM helices of 9.5, 10, 10.5, 11, and 11.5 Å, as described previously (Seubert et al., 2003).

**Online supplemental material.** Fig. S1 shows qRT-PCR of *EVI1* using the Taqman gene expression master mix (Applied Biosystems) and specific primers, as previously described (Vinatzer et al., 2003). In Fig. S2, CD34 $^+$  progenitors cells either from controls or from patients were cultured in methylcellulose in the presence of SCF and various doses of G-CSF, or in the presence of SCF alone. Granulocytic colonies were counted 15 d later. Alternatively, cells from patients were cultured with or without 1  $\mu\text{M}$  AZD1480. Fig. S3 indicates granulocytic differentiation using FACS analysis using anti-CD34, anti-CD15, anti-CD14, and anti-CD11b antibodies. Online supplemental material is available at <http://www.jem.org/cgi/content/full/jem.20090693/DC1>.

We thank all of the patients and the controls who participated in the study, and AstraZeneca for the gift of the JAK2-specific inhibitor (AZD1480). We are grateful to Dr. N. Auger for performing cytogenetic analysis of patient 15, to Dr. C. Bellané-Chantelot for help in the genetic analysis of the pedigree, and to C. Preudhomme for providing us with samples of patients with neutrophilia. We also thank Dr. M. Ito for providing NOG mice.

This work was supported by grants from the Ligue Nationale Contre le Cancer (équipe labelisée 2007), the Institut National du Cancer (INCa; projets libres 2007), the Laurette Fugain Association, and the Institut National de la Santé et de la Recherche Médicale. I. Plo received funds from INCa, Y. Zhang received funds from Medicen, and M. Nakatake received funds from la Ligue Nationale contre le Cancer.

The authors declare no financial conflict of interest.

Submitted: 27 March 2009

Accepted: 30 June 2009

## REFERENCES

Adams, P.D., D.M. Engelman, and A.T. Brunger. 1996. Improved prediction for the structure of the dimeric transmembrane domain of glycoporphin A obtained through global searching. *Proteins*. 26:257–261.

Bhatia, M., J.C. Wang, U. Kapp, D. Bonnet, and J.E. Dick. 1997. Purification of primitive human hematopoietic cells capable of repopulating immunodeficient mice. *Proc. Natl. Acad. Sci. USA*. 94:5320–5325.

Chaligne, R., C. Tonetti, R. Besancenot, L. Roy, C. Marty, P. Mossuz, J.J. Kiladjian, G. Socie, D. Bordessoule, M.C. Le Bousse-Kerdiles, et al. 2008. New mutations of MPL in primitive myelofibrosis: only the MPL W515 mutations promote a G1/S-phase transition. *Leukemia*. 22:1557–1566.

de la Chapelle, A., A.L. Traskelin, and E. Juvonen. 1993. Truncated erythropoietin receptor causes dominantly inherited benign human erythrocytosis. *Proc. Natl. Acad. Sci. USA*. 90:4495–4499.

De Melo, V., M. Vetter, H. Mazzullo, J.D. Howard, D.R. Betts, E.P. Nacheva, J.F. Aupperley, and A.G. Reid. 2008. A simple FISH assay for the detection of 3q26 rearrangements in myeloid malignancy. *Leukemia*. 22:434–437.

Ding, J., H. Komatsu, A. Wakita, M. Kato-Uranishi, M. Ito, A. Satoh, K. Tsuboi, M. Nitta, H. Miyazaki, S. Iida, and R. Ueda. 2004. Familial essential thrombocythemia associated with a dominant-positive activating mutation of the c-MPL gene, which encodes for the receptor for thrombopoietin. *Blood*. 103:4198–4200.

Forbes, L.V., R.E. Gale, A. Pizzey, K. Pouwels, A. Nathwani, and D.C. Linch. 2002. An activating mutation in the transmembrane domain of the granulocyte colony-stimulating factor receptor in patients with acute myeloid leukemia. *Oncogene*. 21:5981–5989.

Germeshausen, M., M. Ballmaier, and K. Welte. 2007. Incidence of CSF3R mutations in severe congenital neutropenia and relevance for leukemogenesis: Results of a long-term survey. *Blood*. 109:93–99.

Ito, M., H. Hiramatsu, K. Kobayashi, K. Suzue, M. Kawahata, K. Hioki, Y. Ueyama, Y. Koyanagi, K. Sugamura, K. Tsuji, et al. 2002. NOD/SCID/ $\gamma\text{c}^{-/-}$  mouse: an excellent recipient mouse model for engraftment of human cells. *Blood*. 100:3175–3182.

James, C., F. Mazurier, S. Dupont, R. Chaligne, I. Lamrissi-Garcia, M. Tulliez, E. Lippert, F.X. Mahon, J.M. Pasquet, G. Etienne, et al. 2008. The hematopoietic stem cell compartment of JAK2V617F-positive myeloproliferative disorders is a reflection of disease heterogeneity. *Blood*. 112:2429–2438.

Kralovics, R., K. Indrak, T. Stopka, B.W. Berman, J.F. Prchal, and J.T. Prchal. 1997. Two new EPO receptor mutations: truncated EPO receptors are most frequently associated with primary familial and congenital polycythemias. *Blood*. 90:2057–2061.

Liu, F., G. Kunter, M.M. Krem, W.C. Eades, J.A. Cain, M.H. Tomasson, L. Hennighausen, and D.C. Link. 2008. Csf3r mutations in mice confer a strong clonal HSC advantage via activation of Stat5. *J. Clin. Invest.* 118:946–955.

Matsumura, T., Y. Kometani, K. Ando, Y. Hirano, I. Katano, R. Ito, M. Shiina, H. Tsukamoto, Y. Saito, Y. Tokuda, et al. 2003. Functional CD5+ B cells develop predominantly in the spleen of NOD/SCID/ $\gamma\text{c}^{-/-}$  (NOG) mice transplanted either with human umbilical cord blood, bone marrow, or mobilized peripheral blood CD34 $^+$  cells. *Exp. Hematol.* 31:789–797.

McLemore, M.L., J. Poursine-Laurent, and D.C. Link. 1998. Increased granulocyte colony-stimulating factor responsiveness but normal resting granulopoiesis in mice carrying a targeted granulocyte colony-stimulating factor receptor mutation derived from a patient with severe congenital neutropenia. *J. Clin. Invest.* 102:483–492.

Panopoulos, A.D., and S.S. Watowich. 2008. Granulocyte colony-stimulating factor: molecular mechanisms of action during steady state and ‘emergency’ hematopoiesis. *Cytokine*. 42:277–288.

Seubert, N., Y. Royer, J. Staerk, K.F. Kubatzky, V. Moucadel, S. Krishnakumar, S.O. Smith, and S.N. Constantinescu. 2003. Active and inactive orientations of the transmembrane and cytosolic domains of the erythropoietin receptor dimer. *Mol. Cell*. 12:1239–1250.

Vinatzer, U., C. Mannhalter, M. Mitterbauer, H. Gruener, H. Greinix, H.H. Schmid, C. Fonatsch, and R. Wieser. 2003. Quantitative comparison of the expression of EVI1 and its presumptive antagonist, MDS1/EVI1, in patients with myeloid leukemia. *Genes Chromosomes Cancer*. 36:80–89.

Wiestner, A., R.J. Schlemper, A.P. van der Maas, and R.C. Skoda. 1998. An activating splice donor mutation in the thrombopoietin gene causes hereditary thrombocythaemia. *Nat. Genet.* 18:49–52.